Comparative Biochemistry and Physiology - Part D: Genomics and Proteomics 58 (2026) 101727

Contents lists available at ScienceDirect

Comparative Biochemistry and Physiology - Part D: Genomics and Proteomics

journal homepage: www.elsevier.com/locate/cbpd

Epitranscriptomic variation in banded newts (*Ommatotriton vittatus*) across life stages and sexes in the semi-arid habitat in northern Israel

Ari Meerson [a,b,*], Monika Almozlino [a], Gad Degani [a,b], Dani Bercovich [a,c]

[a] Faculty of Sciences, Tel-Hai Academic College, Upper Galilee, 1220800, Israel
[b] MIGAL- Galilee Research Institute, Kiryat Shmona, 1101602, Israel
[c] Molecular Genetics Lab, Shamir Research Institute, Katzrin, 1290000, Israel

ARTICLE INFO

Edited by Chris Martyniuk

Keywords:
Amphibians
Life cycle
Metamorphosis
Gene expression
Epitranscriptome
RNA modification

ABSTRACT

The banded newt, *Ommatotriton vittatus*, is considered endangered in Israel, which is the southern border of its distribution and requires adaptation to highly unstable habitats. Banded newts have both aquatic and terrestrial forms, going through metamorphosis and various phenotypic changes during their life. Our group has previously reported on the extensive transcriptomic remodeling based on sex and especially the life stage of the newt. These dramatic changes in gene expression are likely accompanied by extensive epitranscriptomic regulation, which remains poorly understood.

In this study, direct RNA sequencing was used to characterize m^6A RNA modifications in 12 newts from the Nehalit population. We focused on 127 genes with >30 differentially modified regions (DMRs, with a differential modification score > 5) in their transcripts, involved in structural, translational, and extracellular matrix processes. Among them, 18 genes showed clustering of methylation patterns according to life stage, particularly keratins and translation-related proteins, suggesting that m^6A plays a regulatory role in structural remodeling and developmental transitions. In contrast, the majority of DMR genes were associated with housekeeping and stress-response functions and did not show life-stage-specific clustering. Cross-analysis with differential expression data further indicated that muscle, immune, and connective tissue pathways are co-regulated at both the transcriptional and epitranscriptomic levels.

These findings provide the first evidence of m^6A methylation patterns in *O. vittatus* and highlight their role in developmental transitions. The results advance understanding of transcriptomic–epitranscriptomic regulation in amphibian plasticity, and more generally, in vertebrate development.

1. Introduction

Amphibians undergo metamorphosis and live in both aquatic and terrestrial habitats. Amphibians are ectothermic, their skin is permeable to gases and fluids, covered with mucus, serving as a respiratory surface. Amphibians in clade *Caudata*, also known as *Urodele*, have 4 limbs and a tail, with most having a cleavage site at its base.

The banded newt, *Ommatotriton vittatus* (previously *Triturus vittatus*) is divided into 3 subspecies: *O. v. cilicensis* which is located along the northeastern beach of the Mediterranean Sea, *O. v. ophryticus* located in the Caucasus region from the east, and from the south to the Black Sea and *O. v. vittatus*, located in narrow strip along the beach on the eastside of the Mediterranean Sea, from Turkey in the north to Israel in the south (Degani, 2019a). Israel has a diverse topography and a harsh climate, encompassing Mediterranean, semi-arid, and arid regions. The land receives limited rainfall limited to the winter period, with long dry periods for the rest of the year, and generally low humidity. These conditions are challenging for amphibians who depend on water source for their breeding sites. The banded newt is considered an endangered species in Israel (Degani, 2019a).

The **life cycle** of *O. vittatus* in the Nehalit pool (in the upper Galilee) was described in 2019 by Degani (Degani, 2019a; Degani, 2019b). Terrestrial adults hide under rocks and eat small vertebrates. In the winter season with the rain the adults relocate into the winter pond and transform into their aquatic phase (Fig. 1). They change in color from brownish grey to brighter green, their tail thickens and turns to a snapper and the males back crest is elongated. After breeding in the water, the males leave immediately while the females leave only after

* Corresponding author at: MIGAL- Galilee Research Institute, Kiryat Shmona, 1101602, Israel.
E-mail address: arimei@m.telhai.ac.il (A. Meerson).

https://doi.org/10.1016/j.cbd.2025.101727
Received 20 October 2025; Received in revised form 30 November 2025; Accepted 8 December 2025
Available online 9 December 2025

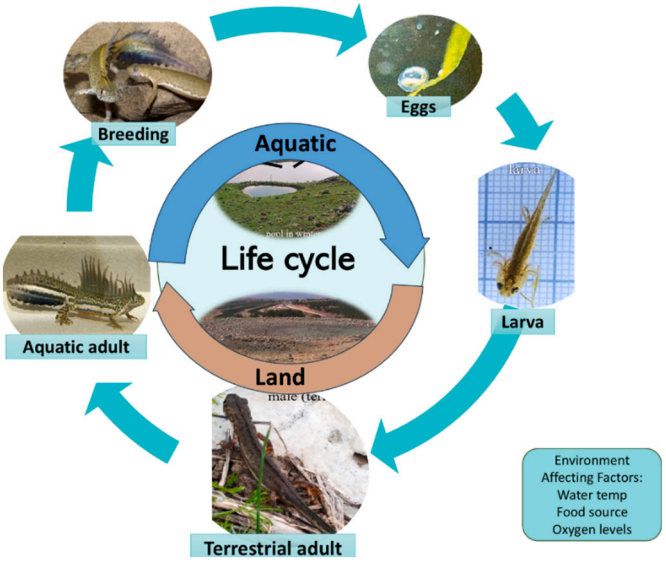

Fig. 1. The life cycle of *Ommatotriton vittatus.*

laying their eggs on plants and rocks in the pond. The eggs hatch, releasing larvae that develop and complete metamorphosis into terrestrial adults (Degani, 2019a).

The length and timing of *O. vittatus* life cycle in Israel was found to be affected by various environmental factors such as food, water temperature and oxygen level of the pool (Pearlson and Degani, 2007; Degani, 2019a; Degani, 2019b).

Temperature and climate mediated development (gene expression sensitive to environmental change) in newts is an important adaptation to environmental changes, including climate change.

Genetic studies described variation in specific genes within and between populations, e.g., **cytochrome *b*eta (**a mitochondrial conserved gene) and **D- loop** (a control region segment known for its evolutionary flexibility) genes (Pearlson and Degani, 2007; Pearlson et al., 2010), mitochondrial markers (**12*S*** and **16*S*** rRNA) and the nuclear rhodopsin gene (***RHO***) (Degani, 2023).

In 2024 Degani and Meerson investigated the **transcriptomic** expression changes across life cycle (aquatic, terrestrial and larva) and sexes (males and females) in the Nehalit Pool newt population. They found ~10 K differentially expressed (DE) genes playing roles in various pathways. Among these, **Uromodulin homolog** genes, linked to **kidney function**, were upregulated in aquatic vs. terrestrial adults, which is consistent with a change in nitrogen excretion in transition from watery to terrestrial environment. Another significant gene, ***DUOXA1*** (Dual Oxidase Maturation Factor 1), involved in thyroid signaling, was elevated in terrestrial phase compared to others. Thyroid hormones hold an important role in triggering **metamorphosis** in amphibians. Additional developmental and metabolic pathways were overrepresented among DE genes, including epidermis development, nervous system development, and nucleotide-sugar biosynthesis, further emphasizing the complexity of molecular changes associated with life cycle transitions. Overall, these findings demonstrated that metamorphosis and environmental transition are associated with major **transcriptomic remodeling.** The largest difference was found between aquatic larvae and aquatic adults, in agreement with the drastic changes associated with metamorphosis. The next largest differences were between terrestrial and aquatic adults, corresponding to adaptation to habitat transition (Degani and Meerson, 2024).

RNA modifications, also known as the "epitranscriptome", refer to chemical modifications that occur on RNA molecules after transcription, influencing their stability, processing, translation efficiency, and function without altering the underlying genetic code. N^6-methyladenosine (**m^6A**) modification is the most prevalent type of RNA regulatory mechanism controlling gene expression in eukaryotes. It involves adding methyl group to Adenosine base of RNA strand by a "writer" protein, a process that can be reversed back to canonical base by "eraser" proteins. m^6A sites are often evolutionary conserved in vertebrates and contain a typical consensus sequence DRACH (D = G, A or U; R = G or A; H = A, C or U). m^6A modification plays a role in many biological processes, from regulating gene expression, and development processes to disease involvement spermatogenesis, embryogenesis, cortical neurogenesis, and carcinogenesis (Roundtree et al., 2017; Huang et al., 2020; Lee et al., 2020).

.In amphibians, knowledge about m^6A remains limited, but recent studies in *Xenopus laevis* provide clear evidence for its functional importance. The first transcriptome-wide mapping of m^6A in *X. laevis* testes revealed that m^6A peaks are enriched near start and stop codons, and exposure to the herbicide atrazine altered approximately 1380 methylation sites. Moreover, global m^6A levels showed a positive correlation with mRNA abundance, indicating a regulatory role in transcript stability and expression (Sai et al., 2020). Another study demonstrated that circRNAs in *X. laevis* testes also carry m^6A modifications and that atrazine exposure significantly altered these methylation profiles, suggesting that the amphibian male germline is highly sensitive to environmental and epitranscriptomic perturbations (Zhang et al., 2023a; Zhang et al., 2023b).

At the developmental level, suppression of *METTL3* in Xenopus embryos disrupted anterior–posterior neural patterning, neural crest specification, and neuronal differentiation. These phenotypes were partially phenocopied by depletion of m^6A readers and mRNA decay factors, linking m^6A-dependent regulation to *WNT* signaling and spatial neural development (Kim and Jang, 2021).

Collectively, these findings indicate that m^6A in amphibians is evolutionarily conserved and plays essential roles in reproduction and embryonic development. Nevertheless, genome-wide analyses of m^6A during metamorphosis and regeneration in other amphibian groups, such as salamanders and newts, are still lacking. While previous research focused on populations in the coastline area and Galilee region of Israel (Pearlson and Degani, 2007; Pearlson and Degani, 2008; Degani, 2019a; Degani and Meerson, 2024), to our knowledge, RNA modifications have not been investigated in banded newts. In this research, we utilized direct RNA sequencing (ONT) to sequence the RNA of the Nehalit banded newt population, investigate the difference in RNA modification (m^6A) between life stages and sexes, and explore the connection between RNA modifications and gene expression.

2. Methods

The overall scheme of methods used in this study is shown in Fig. 2.

2.1. Newt samples from Nehalit

Previously collected newt samples (tail clippings) from Nehalit were retrieved from storage. These samples had been collected by our research group for differential expression (DEG) analysis published previously (Degani and Meerson, 2024). The samples were stored at −80 °C in 1.5-ml tubes containing RNAlater. RNA was extracted from these samples using Tri-reagent (Sigma-Aldrich).

2.2. Sample preparation and transcriptome sequencing

The samples were assessed for RNA integrity using the Agilent 4150 TapeStation and quantified using a DeNovix spectrophotometer. Twelve samples were found to have the quantity and integrity (RNA Integrity Number (RIN) $\geq$ 7) required for sequencing, consisting of 2 terrestrial males, 3 terrestrial females, 3 aquatic males, 1 aquatic female, and 3 larval samples. Direct RNA sequencing was performed on MinION Mk1B and Mk1C devices using RNA flow cells (FLO-MIN004RA) (Fig. 2;

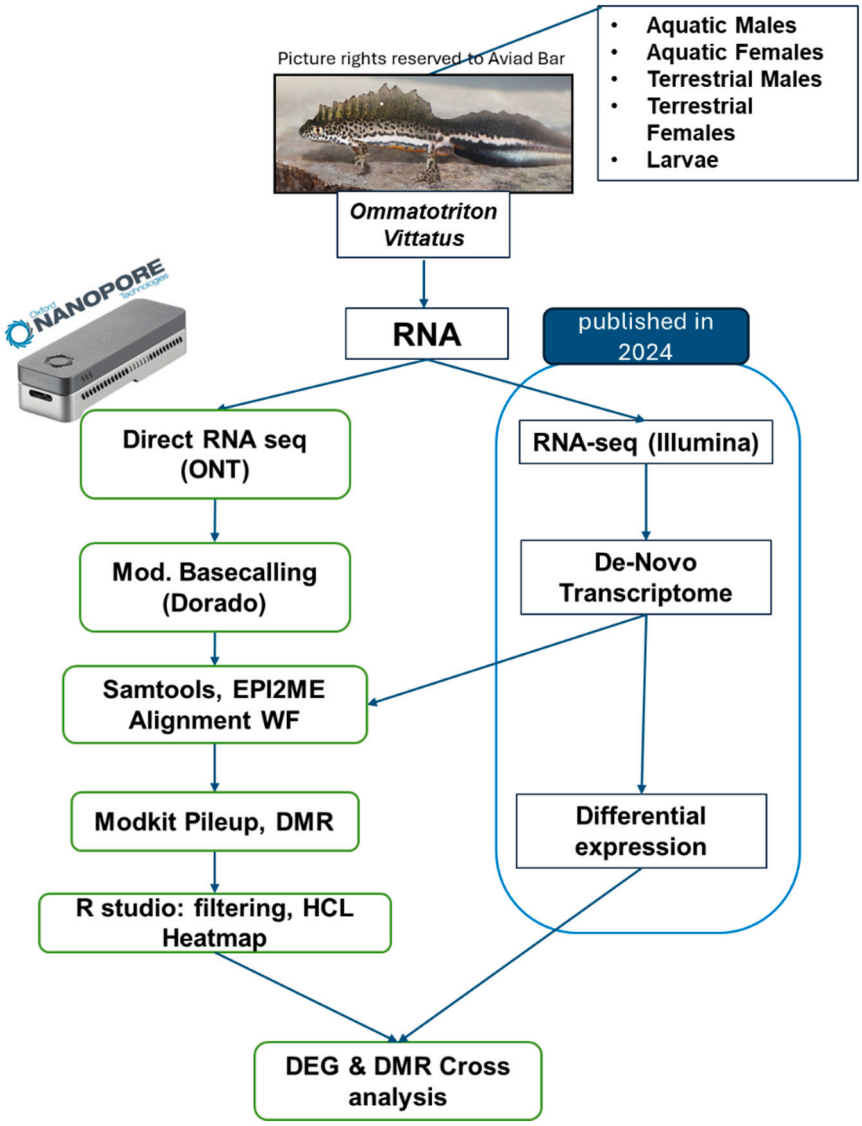

Fig. 2. Scheme of methods used in this study.

Oxford Nanopore Technologies) following the manufacturer's Direct RNA Sequencing protocol (SQK-RNA004) in MinKNOW v.23.07.12 (Oxford Nanopore Technologies, 2023). This approach enables sequencing of both poly(A) + mRNAs and poly(A) + non-coding RNAs (Wang et al., 2021).

2.3. Bioinformatic pipeline and DMR analysis

Base calling was performed on raw sequencing results using the Dorado software v.0.6.0 (Oxford Nanopore Technologies), using an RNA basecalling model that detects methylation of adenosine (m^6A) in the DRACH context (rna004_130bps_sup@v3.0.1). The resulting reads were sorted and aligned to a reference transcriptome (assembled in our 2024 study (Degani and Meerson, 2024)) using Samtools and the Epi2me GUI (Oxford Nanopore Technologies), WF-Alignment workflow. Methylation profiles were generated with the modkit pileup command (Modkit v0.4.1, Oxford Nanopore Technologies), which produced BED files tabulating the positions of m^6A modifications. These files were subsequently visualized using the Integrative Genomics Viewer (IGV).

To detect and analyze regions with differential methylation (DMRs) in pairwise comparisons (based on biological groups), BED files were generated using *modkit dmr pair* (Modkit v0.4.1; parameter: *–base A*). To eliminate noise and false positives, each file was filtered by score > 5, which is a measure of statistical significance representing both the magnitude of methylation difference between two samples and the sequencing coverage. The resulting files were merged into a single CSV dataset. Known genes were annotated by matching IDs in the reference transcriptome with ortholog names in RStudio (v4.4.2). The differential modification region (DMR) dataset was then sorted by frequency of gene occurrence ("CHROM" count) and filtered to retain only genes with >30 occurrences of DMRs. This process yielded the candidate DMR gene list, while unknown genes were excluded from further analysis.

2.4. Heatmap creation

Heatmaps with hierarchical clustering (HCL) were generated for each gene in the DMR list using RStudio. First, Pileup BAM files for each sample were filtered with Bash scripts (WSL2) to retain only DMR-associated genes and their specific positions. In RStudio, low-coverage regions were excluded by removing the lowest 5 % of mean coverage values for each gene individually, as overall coverage levels were high (~8000 reads per gene on average). Filtered files were merged to combine all samples, and gene-specific subsets were prepared. Heatmaps were then constructed using the Pheatmap package, with

clustering performed via Hclust on distance matrices calculated with Gower's distance (packages: Cluster, Dplyr, Tidyr, Pheatmap).

2.5. Classification of genes by HCL

Based on the clustering patterns, genes were divided into two categories: those that clustered according to their biological groups and those that did not. Genes were classified as "Yes" if their clustering contained no more than one sample outside its biological group, and as "No" if more than one such sample was present.

2.6. Gene enrichment

Functional enrichment analysis was performed using g:Profiler (version e113_eg59_p19_f6a03c19) with g:SCS multiple testing correction method, applying a significance threshold of 0.05 (Kolberg et al., 2023). *Homo Sapiens* was used as a reference species due to extensive annotation.

2.7. Venn diagram creation

The filtered (score > 5) DMR files previously generated were used to create 6 DMR datasets (for the desired biological comparisons) in R studio, changed to a list of genes (grouped and counted genes mentioned and compiled them as one with attached ortholog names to the known genes. The unidentified genes were included in the Venn creation using the web tool InteractiVenn (Heberle et al., 2015).

2.8. Cross analysis of DEG and DMR associated genes

The list of 127 DMR-associated genes was cross-analyzed with differential expression results from the transcriptome study (Degani and Meerson, 2024), where DEGs were defined as padj $\leq$0.05, |log2 fold change| $\geq$ 1, and minimum count $\geq$30. The DMR status of each gene was determined from the DMR datasets described above. Genes were considered overlapping if they were both differentially expressed and differentially methylated in the same comparison (Terrestrial vs. Aquatic, Aquatic vs. Larva, Terrestrial vs. Larva). The overlapping genes were compiled into Table 2.

3. Results

To identify the most prominent DMR-associated candidate genes, DMR positions with a score > 5 were sorted by frequency of gene occurrence and filtered to retain only genes with >30 DMRs, while unknown genes were excluded from further analysis. A total of 127 genes were identified as containing >30 DMRs (Table 1 presents a short list; the complete list is provided in Supplementary Table 1). Principal component analysis (PCA) based on modification scores in the DMRs of these 127 genes shows that samples cluster according to biological groups overall, with the larvae showing the most separation from adult samples (Fig. 3A).

To assess the relationship between methylation changes and life stages, hierarchical clustering (HCL) of samples was performed for each of the 127 candidate genes. This yielded two categories of genes: those that clustered according to biological groups and those that did not. Representative genes include *KRT12, KRT15*, and *TIMP1* from the first category, and *CLEC2D, COL1A2*, and *ACTG2* from the second (Fig. 3B). In addition, pathway enrichment was performed on both gene lists. Full gene lists for both groups are provided in Supplementary Table 2.

Eighteen genes clustered according to biological conditions. These included keratin-associated genes (*KRT12, KRT15*), protein translation genes (*EEF2, EIF1*), extracellular matrix and tissue remodeling genes (*COL6A1, TIMP1, MYL12B, ENO1*). This group was enriched in structural and translation-related functions, particularly keratin and ribosomal proteins (Fig. 4A).

Table 1
most frequent DMR genes - all groups' comparisons (short list). DMR positions with a score > 5 were sorted by frequency of gene occurrence and filtered to retain only genes with >30 DMRs. the complete list of 127 genes is provided in Supplementary Table 1.

Gene ortholog name	Count
CLEC2D	1775
KRT12	295
COL1A2	217
KRT15	185
YWHAB	137
EEF2	179
KRT76	178
ACTG2	173
HSPA8	167
EEF1G	122
SPACA4	109
RPL36	105
MYL1	104
RPS12	98
TUBA1B	97
RPL13	95
*epidermal diff**	49
thdl17	45
EF1α-F2	94
COL1A1	383
RPS11	88
RPS17	88
RPL6	86
CRISP3	84
RPLP1	107
GAPDH	83
NSA2	83
HMGB2	82
CFL1	79
MYLPF	95

The remaining 109 genes did not cluster according to biological condition. This group included constitutively expressed genes (*GAPDH, ACTG2*), heat shock proteins (*HSPA8, HSP90AB1*), RNA-binding and splicing factors (*HNRNPK, EIF4A1*), oxidative stress–related genes (*GPX4, PRDX5*), mitochondrial and metabolic genes (*COX7B, PDIA3*), and cytoskeleton/muscle contraction genes (*MYL1, CKM, TNNI2*). Enrichment analysis indicated that this group was primarily associated with translation and ribosome-related pathways (Fig. 4B).

So far, differences in mRNA methylation were examined across all groups combined. Next, specific biological comparisons were investigated separately, including comparisons based on sex and on life stage. A Venn diagram was constructed to illustrate the overlap of differentially methylated genes (DMRs) among the six pairwise comparisons (Fig. 5); the gene list was not filtered by the number of DMRs per gene, but included DMRs with score > 5. In total, 43 genes were found to be differentially methylated across all comparisons, of which 32 were annotated as known genes. The gene list is provided in Supplementary Table 3. Gene enrichment analysis of these 32 genes revealed significant overrepresentation of translational machinery, such as ribosomal subunits, rRNA processing, and eukaryotic translation elongation (g.profiler summary outputs are provided in Supplementary Fig. 1). The highest number of unique DMR genes was identified in the comparison of Terrestrial Males vs Aquatic Males (459 genes), suggesting extensive life stage-specific mRNA modification associated with the transition from land to water in males. In contrast, the analogous comparison in females revealed only 29 unique genes, indicating a more limited modification pattern.

3.1. Link between DE and DMR

To explore the relationship between RNA modifications and gene expression, the list of 127 DMR-associated genes was cross-analyzed

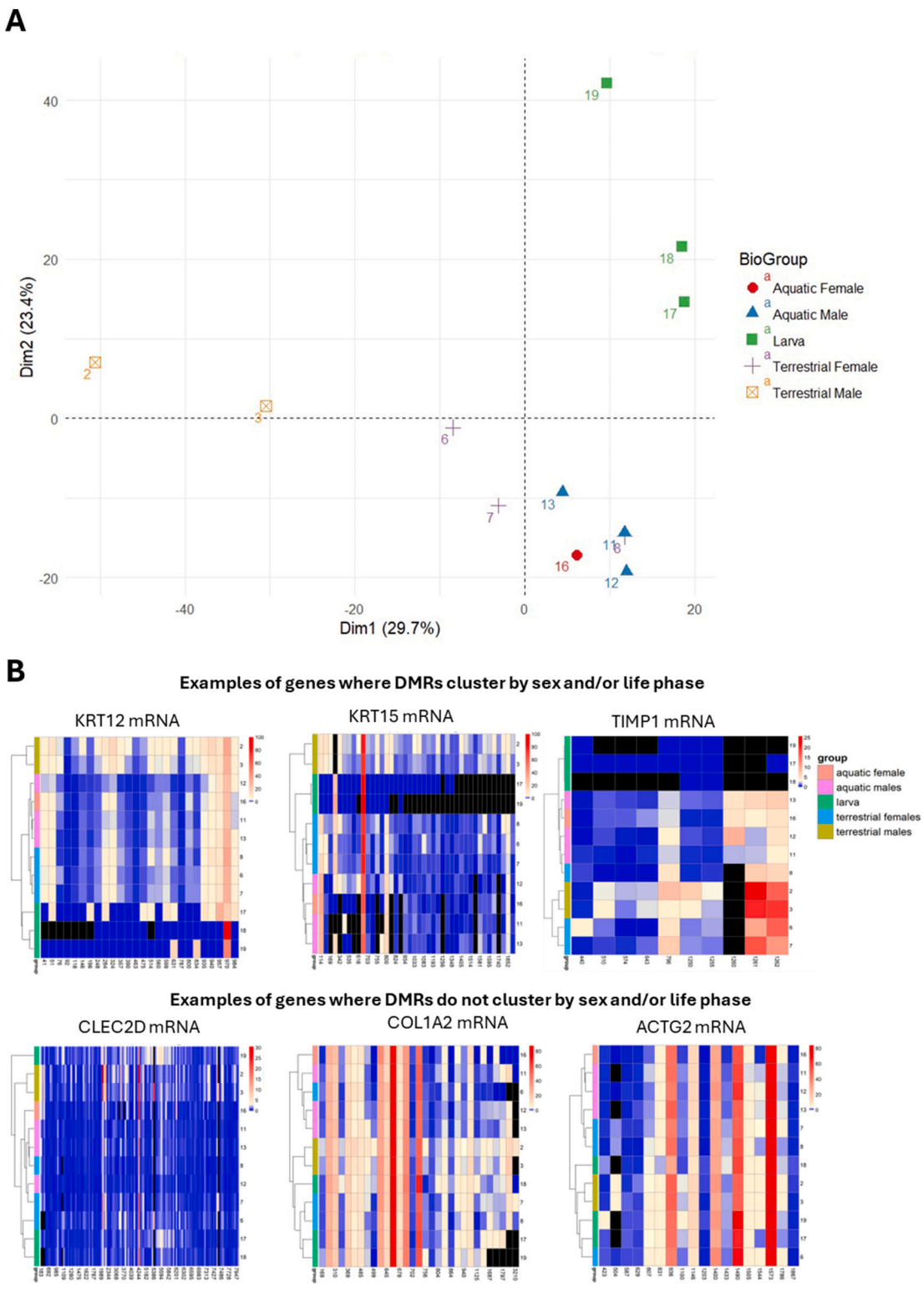

Fig. 3. A. PCA plot based on m^6A modification levels in the DMRs of the transcripts of 127 highest DMR-containing genes. B. Heatmaps of m^6A methylation percentage with hierarchical clustering across mRNA**s.** Heatmaps depict m^6A methylation (%) for each gene across different DMR positions (x-axis) and samples (y-axis). Samples are organized into five biological groups representing different life stages and sexes: aquatic females, aquatic males, larvae, terrestrial females, and terrestrial males, indicated by color codes on the right of each panel (cyan, blue, purple, pink, and green, respectively). Each column represents an individual sample, and each row corresponds to a methylated peak detected along the transcript. The heatmap color gradient from blue (low) to red (high) reflects the relative methylation percentage at each locus, while black cells indicate missing or undetectable signal.

A. DMR associated genes which cluster according to bio groups enrichment analysis

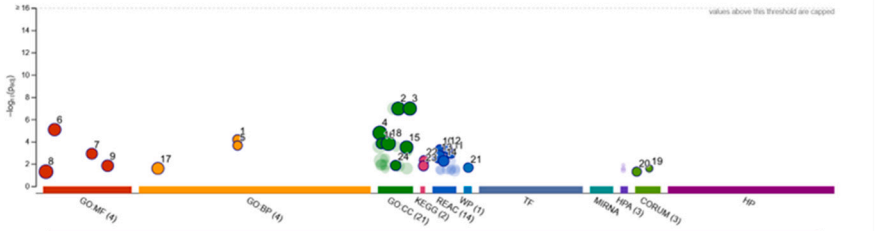

ID	Source	Term ID	Term Name	p_{adj} (query_1)
1	GO:BP	GO:0045104	intermediate filament cytoskeleton organization	6.455×10^{-5}
2	GO:CC	GO:0065010	extracellular membrane-bounded organelle	1.073×10^{-7}
3	GO:CC	GO:1903561	extracellular vesicle	1.067×10^{-7}
4	GO:CC	GO:0005615	extracellular space	1.637×10^{-5}
5	GO:BP	GO:0045109	intermediate filament organization	2.228×10^{-4}
6	GO:MF	GO:0005198	structural molecule activity	8.321×10^{-6}
7	GO:MF	GO:0045296	cadherin binding	1.206×10^{-3}
8	GO:MF	GO:0003723	RNA binding	4.933×10^{-2}
9	GO:MF	GO:0050839	cell adhesion molecule binding	1.448×10^{-2}
10	REAC	REAC:R-HSA-15...	Eukaryotic Translation Elongation	5.110×10^{-4}
11	REAC	REAC:R-HSA-96...	SARS-CoV-1-host interactions	1.140×10^{-3}
12	REAC	REAC:R-HSA-15...	Peptide chain elongation	4.290×10^{-4}
13	REAC	REAC:R-HSA-12...	Developmental Biology	2.299×10^{-3}
14	REAC	REAC:R-HSA-68...	Keratinization	5.366×10^{-3}
15	GO:CC	GO:0099080	supramolecular complex	3.169×10^{-4}
16	GO:CC	GO:0005882	intermediate filament	1.465×10^{-4}
17	GO:BP	GO:0006412	translation	2.532×10^{-2}
18	GO:CC	GO:0031982	vesicle	1.475×10^{-4}
19	CORUM	CORUM:5266	TNF-alpha/NF-kappa B signaling complex 6	2.484×10^{-2}
20	CORUM	CORUM:306	Ribosome, cytoplasmic	4.938×10^{-2}
21	WP	WP:WP477	Cytoplasmic ribosomal proteins	2.139×10^{-2}
22	KEGG	KEGG:05150	Staphylococcus aureus infection	4.756×10^{-3}
23	KEGG	KEGG:04915	Estrogen signaling pathway	1.501×10^{-2}
24	GO:CC	GO:0044391	ribosomal subunit	1.354×10^{-2}

B. DMR associated genes which don't cluster according to bio groups enrichment analysis

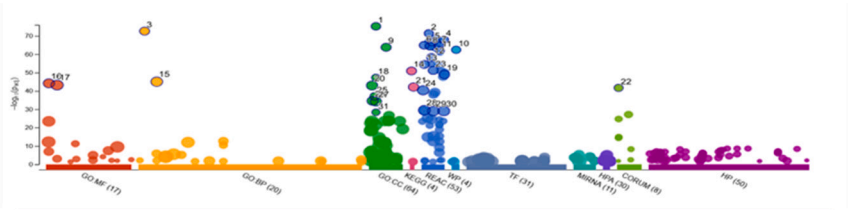

ID	Source	Term ID	Term Name	p_{adj} (query_1)
1	GO:CC	GO:0022626	cytosolic ribosome	5.906×10^{-76}
2	REAC	REAC:R-HSA-15...	Eukaryotic Translation Elongation	4.013×10^{-72}
3	GO:BP	GO:0002181	cytoplasmic translation	2.319×10^{-73}
4	REAC	REAC:R-HSA-19...	Viral mRNA Translation	9.852×10^{-69}
5	REAC	REAC:R-HSA-15...	L13a-mediated translational silencing of Cerulopla...	2.092×10^{-67}
6	REAC	REAC:R-HSA-72...	Cap-dependent Translation Initiation	1.257×10^{-65}
7	REAC	REAC:R-HSA-96...	Response of EIF2AK4 (GCN2) to amino acid deficie...	1.771×10^{-65}
8	REAC	REAC:R-HSA-72...	GTP hydrolysis and joining of the 60S ribosomal s...	4.889×10^{-65}
9	GO:CC	GO:0044391	ribosomal subunit	1.552×10^{-64}
10	WP	WP:WP477	Cytoplasmic ribosomal proteins	3.725×10^{-63}
11	REAC	REAC:R-HSA-17...	SRP-dependent cotranslational protein targeting t...	6.350×10^{-63}
12	REAC	REAC:R-HSA-16...	Influenza Viral RNA Transcription and Replication	5.112×10^{-59}
13	REAC	REAC:R-HSA-97...	Cellular response to starvation	3.351×10^{-55}
14	KEGG	KEGG:03010	Ribosome	1.323×10^{-51}
15	GO:BP	GO:0006412	translation	9.273×10^{-46}
16	GO:MF	GO:0003735	structural constituent of ribosome	7.009×10^{-45}
17	GO:MF	GO:0005198	structural molecule activity	6.456×10^{-44}
18	GO:CC	GO:0022625	cytosolic large ribosomal subunit	5.859×10^{-48}
19	REAC	REAC:R-HSA-72...	rRNA processing	1.109×10^{-49}
20	GO:CC	GO:0005840	ribosome	1.156×10^{-43}
21	KEGG	KEGG:05171	Coronavirus disease - COVID-19	7.566×10^{-43}
22	CORUM	CORUM:306	Ribosome, cytoplasmic	2.168×10^{-42}
23	REAC	REAC:R-HSA-67...	Major pathway of rRNA processing in the nucleolu...	6.555×10^{-52}
24	REAC	REAC:R-HSA-42...	Axon guidance	4.542×10^{-41}
25	GO:CC	GO:0015934	large ribosomal subunit	8.591×10^{-38}
26	GO:CC	GO:0005925	focal adhesion	2.686×10^{-35}
27	GO:CC	GO:0030055	cell-substrate junction	6.297×10^{-35}
28	REAC	REAC:R-HSA-22...	Cellular responses to stress	3.164×10^{-30}
29	REAC	REAC:R-HSA-89...	Metabolism of RNA	9.343×10^{-30}
30	REAC	REAC:R-HSA-98...	Viral Infection Pathways	9.717×10^{-30}
31	GO:CC	GO:0022627	cytosolic small ribosomal subunit	4.299×10^{-29}

Fig. 4. Gene enrichment analysis for 18 DMR-associated genes which cluster according to biological groups (**A**) and those 109 that do not (**B**).

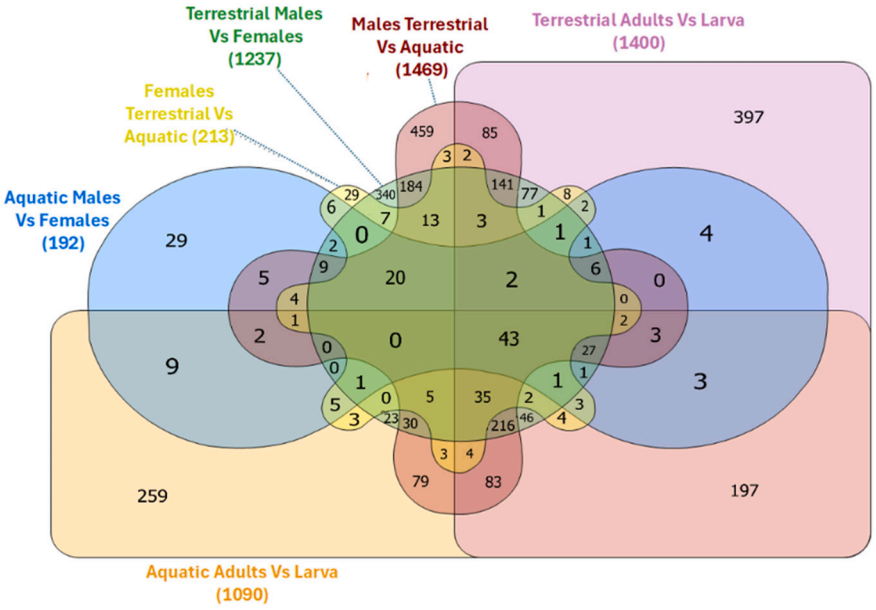

Fig. 5. Venn diagram of genes with differential m^{6}A methylation across six pairwise comparisons.

with differential expression across 3 comparisons (Table 2). Genes that were both differentially methylated and differentially expressed in the same comparison were identified and used for functional enrichment analysis (g.profiler summary outputs are provided in Supplementary Figs. 2–4).

In the **Terrestrial vs. Aquatic** comparison, eight genes showed both DMRs and differential expression (Fig. 6A). These included cytoskeleton and muscle-related genes (*MYH1, KRT15, KRT12*), immune system–related genes (*TIMP1, CRISP3, LGALS4, PPIA*), and a ribosomal gene (*RPS3*). Enrichment analysis indicated overrepresentation of extracellular regions, including extracellular space, secretory granules, and vesicle-related components.

In comparison of **Aquatic Vs Larva** groups, 30 genes showed both DMRs and differential expression (Fig. 6B). These included immune-related genes (*PPIA, LGALS4, IFITM3, MGST3*), muscle and connective tissue genes (*MYH1, NEB, ACTG2, TNNI2, MYLPF, KRT12, KRT15*), ribosomal proteins (*RPS3, RPS3A*), energy homeostasis genes (*CKM, NT5C1B*), and detoxification/oxidative stress–related genes (*GSTT1, S100A11*). Enrichment analysis indicated strong representation of muscle contraction and motor protein pathways, extracellular matrix organization, and ribosomal subunits.

In comparison of **Terrestrial Vs Larva** groups, 27 genes showed both DMRs and differential expression (Fig. 6C). These included immune-related genes (*PPIA, LGALS4, MGST3*), muscle and connective tissue genes (*MYH1,NEB, ACTG2, MYLPF, KRT15*), energy homeostasis (*NT5C1B, CKM*) and detoxification/oxidative stress response genes (*GSTT1*). Enrichment analysis revealed strong representation of muscle structure and contraction pathways, extracellular components, and structural molecular activity.

We then compared the lists of genes that are both differentially expressed and show DMRs in their transcripts, in the three comparisons between life stages (Fig. 6D). 21 genes appeared in both Aquatic vs. Larva and in Terrestrial vs. Larva comparisons, which represented the majority of such genes in both comparisons (30 and 27, respectively), in agreement with the assumption that metamorphosis involves the most significant transcriptomic and epi-transcriptomic changes.

To assess the qualitative relationship between m^{6}A methylation and the abundance of the transcript, we checked whether an increase in m^{6}A methylation in DMRs correlates with an increase, or decrease, in expression, in the subset of genes identified as showing both DMRs in their transcripts and differential expression. We found groups of genes that followed both of these patterns, and additionally, genes which showed increased m^{6}A methylation in some DMRs and decrease in m^{6}A methylation in other DMRs, among both up- and down-regulated genes (Fig. 7; detailed information is provided in Supplementary Tables 4–5).

Table 2
DE and DMR genes of 3 separate comparisons. *epidermal diff.* denotes "epidermal differentiation-specific protein-like".

TR vs Aq	Aq vs Larva	Tr vs Larva
CRISP3	*ACTG2*	*ACTG2*
*Epidermal diff**	*CKM*	*CKM*
KRT12	*COL3A1*	*COL3A1*
KRT15	*DSP*	*DSP*
MYH1	*Epidermal diff**	*Epidermal diff**
PPIA	*GSTT1*	*GSTT1*
RPS3	*IUNH*	*IUNH*
TIMP1	*KRT15*	*KRT15*
	LGALS4	*LGALS4*
	MGST3	*MGST3*
	MYH1	*MYH1*
	MYL1	*MYL1*
	MYLPF	*MYLPF*
	NEB	*NEB*
	NT5C1B	*NT5C1B*
	POSTN	*POSTN*
	PPIA	*PPIA*
	SPACA4	*SPACA4*
	TNNC2	*TNNC2*
	TNNI2	*TNNI2*
	YWHAB	*YWHAB*
	BGN	*COL2A1*
	ENO3	*FABP4*
	IFITM3	*NSA2*
	KRT12	*RPL9*
	RPS10	*RPS2*
	RPS3	*SUGP2*
	RPS3A	
	S100A11	
	TIMP1	

4. Discussion

This study represents the first analysis of m^{6}A RNA methylation in the banded newt (*Ommatotriton vittatus*) and provides new insight into how life stage and sex differences may influence epitranscriptomic

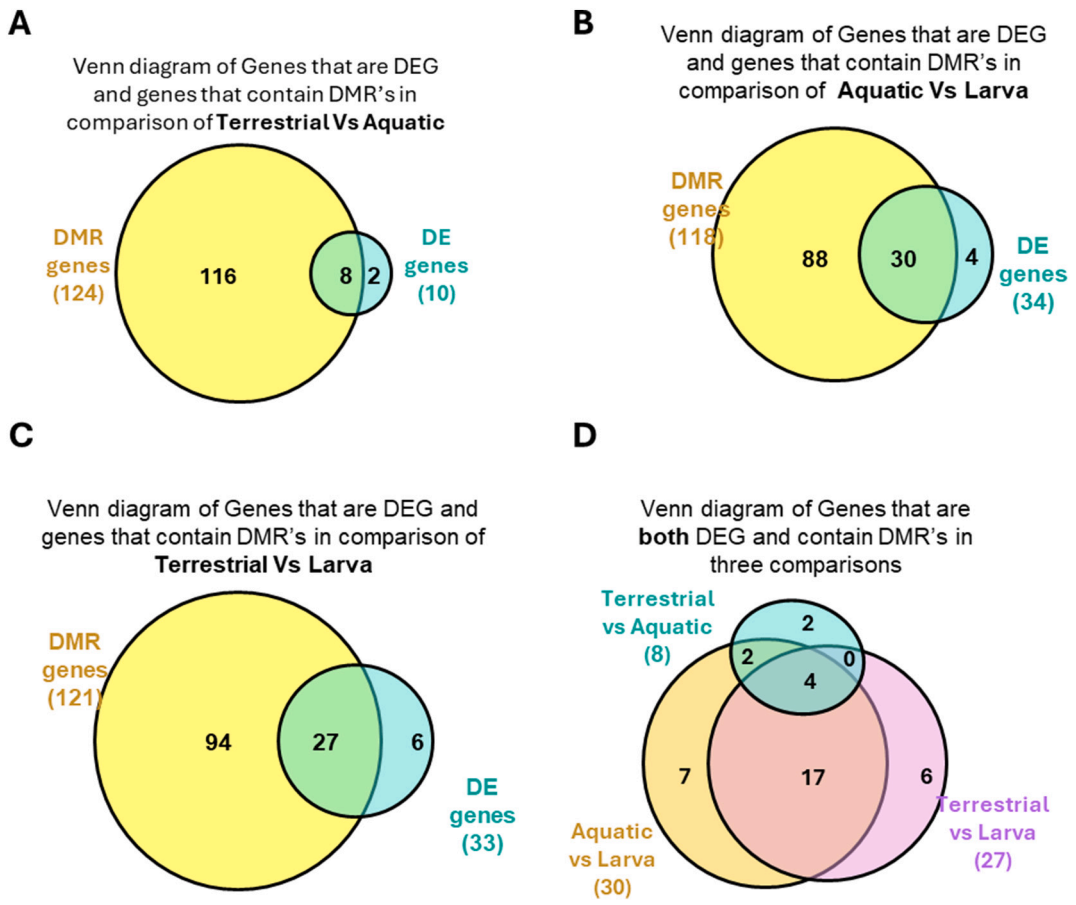

Fig. 6. (A-C) Venn diagrams of genes that are DEG and genes that contain DMRs in their transcripts, by comparison. A: Terrestrial Vs Aquatic, B: Aquatic vs. Larva, C: Terrestrial vs. Larva. D: Venn diagram of genes that are both DEG and contain DMRs in their transcripts, in all comparisons.

variation. Using direct RNA sequencing, we successfully detected and quantified m^6A modifications in the transcriptomes of 12 newts from the Nehalit population. From this dataset, 127 candidate genes were identified as containing multiple differentially modified regions (DMRs) in their transcripts, including genes involved in structural organization, translation, and extracellular matrix processes. These categories are consistent with the physiological changes observed during metamorphosis and habitat transition, which involve remodeling of skin and connective tissue.

Of the DMR-associated genes, 18 showed clustering of methylation patterns according to life stages. These included keratins and translation-related proteins, highlighting the involvement of m^6A modifications in regulating structural processes and supporting stage-specific morphological changes; examples are discussed below. In contrast, the majority of DMR genes did not cluster according to biological state. These were largely housekeeping, stress response, and RNA-binding genes, indicating that methylation also plays a role in general maintenance and homeostasis pathways that operate independently of life stage.

Thus, in *KRT12* mRNA, methylation levels were distinctly clustered by life stage. Larvae and aquatic individuals exhibited high, uniform methylation, while terrestrial adults displayed a heterogeneous pattern with reduced overall m^6A intensity. This suggests that m^6A methylation in keratin 12 is associated with epithelial and skin restructuring during transition from aquatic to terrestrial environments. The *KRT15* mRNA heatmap shows more variable and localized methylation, with terrestrial individuals showing strong hypermethylation at specific regions. This pattern points to stage-specific regulation of keratin 15, a cytoskeletal protein involved in epithelial renewal and mechanical adaptation.

In *TIMP1* mRNA, which encodes a tissue inhibitor of metalloproteinases, there was clear separation between larval and terrestrial groups, with terrestrial males showing extensive hypermethylation. The increased m^6A signal in adults suggests that m^6A may control extracellular matrix turnover during metamorphic remodeling. By contrast, *CLEC2D* mRNA, a gene associated with immune recognition, showed overall low and stable methylation levels with no significant clustering among groups. This stability implies a constitutive expression pattern that is not strongly modulated by habitat or sex.

M^6A methylation in *COL1A2* mRNA, encoding collagen type I alpha 2, showed a strong contrast between aquatic/larval and terrestrial samples. Terrestrial individuals exhibited higher methylation intensity, consistent with the structural demands of terrestrial life and the need for strengthened connective tissues. Finally, *ACTG2* mRNA, which encodes smooth-muscle actin γ-2, showed a progressive increase in m^6A methylation from larval and aquatic stages to terrestrial adults. This gradient likely reflects the increasing importance of muscle contractility and support for terrestrial locomotion.

Together, these examples represent a category of *O. vittatus* transcripts, in which m^6A methylation patterns are primarily life stage -dependent. Genes related to tissue structure (keratins, collagen, actin) and extracellular remodeling (*TIMP1*) showed strong and coordinated epitranscriptomic variation, while immune-related genes remained relatively constant. The hierarchical clustering across samples highlights that methylation landscapes correspond to ecological phase—aquatic versus terrestrial—more than to sex. These findings support the hypothesis that m^6A serves as a dynamic regulatory layer orchestrating transcriptomic reprogramming during the amphibian life cycle, facilitating physiological adaptation to changing environmental conditions and developmental states.

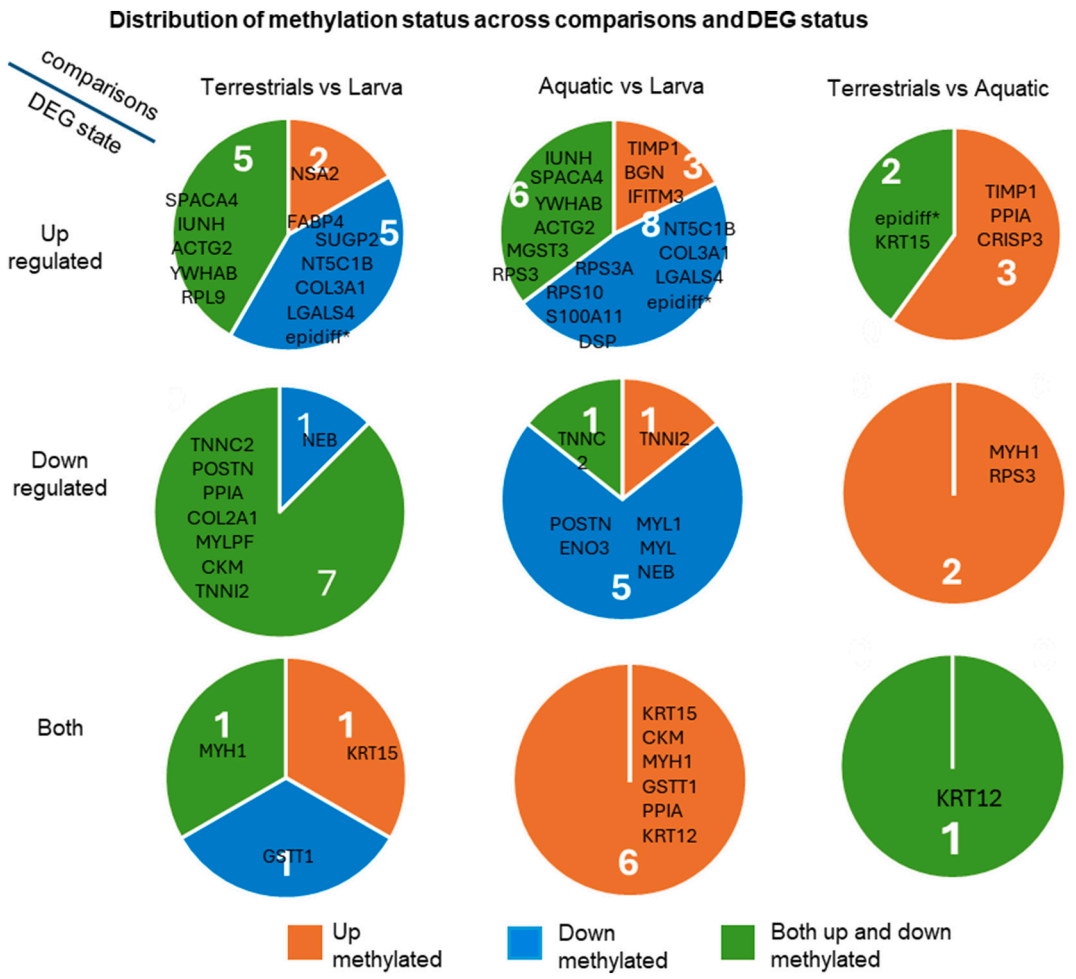

Fig. 7. Distribution of methylation status across comparisons and DEG status, in 38 genes that are both differentially expressed and show DMRs in their transcripts. Genes that are both up- and down-regulated (bottom row) refers to those which have both up- and down-regulated transcripts in the relevant comparison. Genes that are both up- and down-methylated (green) refers to those which show both increased and decreased m^{6}A methylation in different DMRs on their transcripts in the relevant comparison. The numbers of genes in each group are in white, and the gene names are listed.

We further focused on genes showing DMRs in specific comparisons (aquatic vs. terrestrial adults, terrestrial adults vs larvae, aquatic adults vs larvae). The 43 genes which showed DMRs across all six comparisons were over-represented in ribosomal and translation-related categories. This suggests a consistent role for m^{6}A in regulating core cellular machinery. A striking difference was observed between sexes: terrestrial vs. aquatic males showed 459 unique DMR genes, while the same comparison in females yielded only 29, suggesting that males undergo a more extensive epitranscriptomic shift during the land–water transition. This molecular pattern is consistent with the males' more pronounced phenotypical changes during the aquatic phase, such as the development of a prominent dorsal crest, compared to the relatively subtle changes observed in females (Degani, 2019a). Such sex-biased epitranscriptomic variation has not been previously documented in amphibians, but similar male-biased transcriptional plasticity has been described in *Xenopus* gonadal studies, where sex hormone signaling interacts with RNA modifications to drive reproductive functions (Yaoita and Brown, 1990; Shi et al., 1998). Beyond *Xenopus*, genomic resources for urodele amphibians such as *Pleurodeles waltl* (ribbed newt) provide strong frameworks for investigating regeneration and developmental gene regulation (Elewa et al., 2017; Yassouf et al., 2025). Although these studies have not mapped m^{6}A profiles across life stages, they emphasize the importance of large-scale transcriptome remodeling during processes like limb regeneration, which—like metamorphosis—require tight coordination between transcriptional and post-transcriptional mechanisms. Our results in *O. vittatus* suggest that m^{6}A is a candidate regulatory layer in these processes and should be explored in salamanders, which are established regeneration models (McCusker and Gardiner, 2011; Faisal et al., 2024). Modern salamander datasets—especially in *P. waltl*—offer improved transcriptome assemblies and genome resources for regeneration biology. While these works do not present life-stage m^{6}A maps, they give high-quality references (annotations, isoforms) that would make MeRIP-seq or direct RNA m^{6}A calling feasible across stages or tissues (Elewa et al., 2017; Yassouf et al., 2025). The *Axolotl* literature likewise centers on regeneration and epigenetic regulation broadly (DNA methylation, histone marks, miRNAs), but again not on epitranscriptomic variation across life stages (McCusker and Gardiner, 2011; Faisal et al., 2024). Several *X. laevis* studies showed that m^{6}A is present and condition-dependent in amphibians. Testis m^{6}A-seq (including circRNA-m^{6}A) showed robust and differentially modified peaks, including responses to the endocrine disruptor atrazine—strong proof of concept for amphibian m^{6}A mapping and differential analysis, even though these were tissue/condition comparisons rather than life-stage comparisons (Sai et al., 2020; Zhang et al., 2023a; Zhang et al., 2023b). More broadly, metamorphosis in amphibians is orchestrated by thyroid hormone (TH) signaling, which drives large, stage-specific transcriptional programs. This provides a strong a priori rationale for expecting life-stage shifts in m^{6}A, even if they have not yet been charted in newts [18, 19, 24].

Cross-analysis of differential expression and methylation confirmed

that certain genes are regulated at both levels. In terrestrial vs. Aquatic adults, only eight DE + DMR genes were identified, mostly linked to structural and immune functions. By contrast, the larva–adult comparisons (both terrestrial and aquatic) revealed a larger gene set, with 17 genes appearing in both. These were strongly enriched in muscle, connective tissue, and immune-associated pathways, suggesting that the transition from larva to adult involves a direct link between methylation and expression in key developmental processes.

To look for additional evidence of differential m6A methylation of the candidate transcripts we identified, we compared our gene lists with the list of transcripts showing differential m^{6}A methylation in *X. laevis* cells with FTO knockdown (GSE167139 (Kim et al., 2021),), using m^{6}A-Atlas v2.0 DMR download page, exomePeak2 results (https://rnamd.org/m6a/). Three genes in our top 127 DMR list appeared in the FTO knockdown DMR dataset (*EIF5*, *RPL13*, and *RPL6*); so did an additional gene, *DSP,* which was both DE and DMR in our Aquatic adult vs. Larva comparison. Our result support the notion that differential m^{6}A methylation of these genes' transcripts in amphibians has physiological and developmental significance.

Overall, our findings indicate that m^{6}A modifications in *O. vittatus* development are not randomly distributed but instead target specific groups of transcripts. Structural, translational, and immune pathways appear particularly sensitive to methylation changes. Meanwhile, many housekeeping and stress-response genes also carried DMRs, pointing to a broader role for m^{6}A in cellular processes. Together, these results demonstrate that epitranscriptomic modifications add an important regulatory layer to the transcriptomic remodeling already described in this species, and probably contribute significantly to the phenotypic plasticity that underpins amphibian adaptation.

Our study is limited by a small sample size, especially for some subgroups (e.g. only one aquatic female could be sampled), due to the newts' endangered status in Israel. This reduces statistical power, and calls for caution in the generalization of conclusions. Specifically, we expect that the number of transcripts where the m^{6}A pattern clusters according to biological group would increase with higher signal to noise ratios enabled by larger datasets. Additionally, our findings would benefit from future validation by other methods, both analytical (focusing on quantification of specific m^{6}A sites) and functional (e.g. in vitro studies of the mechanisms linking the expression of specific transcripts with their modifications).

When compared to other amphibians, the data from *O. vittatus* reveal both commonalities and distinctions. In *X. laevis*, m^{6}A profiling of testis RNA demonstrated widespread and condition-dependent modifications, with dynamic responses to environmental stressors such as endocrine disruptors (Sai et al., 2020; Zhang et al., 2023a; Zhang et al., 2023b). These studies showed that amphibian m^{6}A marks are not static but vary according to developmental or physiological context. Similarly, desiccation studies in *X. laevis* revealed plastic changes in RNA methylation under stress (Rehman et al., 2024), suggesting that amphibian epitranscriptomes are highly responsive to both endogenous developmental signals and environmental cues.

Our findings illustrate the complex landscape of RNA modifications influencing phenotypic plasticity and adaptability, in the newt as a model animal, and more generally, in vertebrate development. The banded newt is categorized as an endangered species in Israel (Gafny, 2004) and is affected by man-made environmental (agricultural and city development) changes, as well as climate change (Pearlson, 2012). A deeper mechanistic characterization of adaptation processes in this species may aid in conservation efforts, as well as broaden the understanding of vertebrate development and evolution.

CRediT authorship contribution statement

Ari Meerson: Writing – review & editing, Visualization, Supervision, Resources, Project administration, Methodology, Investigation, Formal analysis, Data curation, Conceptualization. **Monika Almozlino:** Writing – review & editing, Writing – original draft, Visualization, Methodology, Investigation, Formal analysis, Data curation. **Gad Degani:** Writing – review & editing, Supervision, Resources, Funding acquisition, Conceptualization. **Dani Bercovich:** Writing – review & editing, Supervision, Resources, Project administration, Funding acquisition.

Funding

This research was funded by internal grants from MIGAL and Tel Hai.

Declaration of competing interest

The authors declare that they have no known competing financial interests or personal relationships that could have appeared to influence the work reported in this paper.

Acknowledgements

The authors thank the administration and personnel of the Tel Hai campus in Katzrin for providing a temporary setting for the work described in this manuscript, during a period of evacuation; and to Taharah Meerson for first suggesting that temporary setting.

Appendix A. Supplementary data

Supplementary data to this article can be found online at https://doi.org/10.1016/j.cbd.2025.101727.

Data availability

Basecalled nanopore sequence reads (in bam format) are deposited in the SRA (BioProject PRJNA990561). The assembled reference transcriptome file is available upon request from the authors.

References

Degani, G., 2019a. The fire Salamandra (Salamandra infraimmaculata) and the banded newt (Triturus vittatus) along the southern border of their distribution. http://www.scirp.org.

Degani, G., 2019b. Ecological and genetic variation of the distribution of various species of amphibians at the southern border of their distribution. Int. J. Plant Anim. Environ. Sci. https://doi.org/10.21276/Ijpaes.

Degani, G., 2023. The genetic diversity of Triturus vittatus vittatus (synonym Ommatotriton vittatus) along the southern border of its distribution. In: Advanced research in biological science, 2. B P international, pp. 102–112. https://doi.org/10.9734/bpi/arbs/v2/5918b.

Degani, G., Meerson, A., 2024. Transcriptome variation in banded newt (Ommatotriton vittatus) during its life cycle and habitat transition. Comp. Biochem. Physiol. D: Genomics Proteomics 50. https://doi.org/10.1016/j.cbd.2024.101203.

Elewa, A., Wang, H., Talavera-López, C., Joven, A., Brito, G., Kumar, A., Tanaka, E.M., 2017. Reading and editing the Pleurodeles waltl genome reveals novel features of tetrapod regeneration. Nat. Commun. 8, 2286.

Faisal, I., Wang, L., Chiu, I., et al., 2024. Epigenetic regulation of regeneration in the axolotl. Regeneration 11 (1), 1–12.

Gafny S. (2004). Threatened amphibians of Israel. In: Dolev A, Perevolotsky A (Eds.) Endangered Species in Israel: Red List of Threatened Animals. Vertebrates. Nature and Park Authority and the Society for the Preservation of Nature, Pub. 55–68.

Heberle, H., M. G. V., da S. F. R., T. G. P., M. R., 2015. InteractiVenn: a web-based tool for the analysis of sets through Venn diagrams. BMC Bioinformatics *16*, 169.

Huang, H., et al., 2020. M^{6}A modification in coding and non-coding RNAs: roles and therapeutic implications in cancer. Cancer Cell 37 (3).

Kim, H., Jang, S., 2021. *METTL3*-mediated m^{6}A modification controls neural patterning and WNT signaling in Xenopus embryos. Mol. Cell. Biol. 41 (12) (e00231-21).

Kim, H., Lee, Y., Kim, S.M., Jang, S., Choi, H., Lee, J.W., Kim, T.D., Kim, V.N., 2021. RNA demethylation by *FTO* stabilizes the *FOXJ1* mRNA for proper motile ciliogenesis. Dev. Cell 56 (8), 1118–1130.e6.

Kolberg, L., Raudvere, U., Kuzmin, I., Adler, P., Vilo, J., Peterson, H. (2023) g: Profiler—interoperable web service for functional enrichment analysis and gene identifier mapping (2023 update) *Nucleic Acids Research. 2023.*

Lee, Y., Choe, J., Park, O.H., Kim, Y.K., 2020. Molecular mechanisms driving mRNA degradation by m^{6}A modification. Trends Genet. 36 (3), 188.

McCusker, C., Gardiner, D.M., 2011. The axolotl model for regeneration and aging research: a mini-review. Gerontology 57 (6), 565–571.

Pearlson, O., 2012. Ecology and Genetic Variance of Banded Newt in Northern Israel.

Pearlson, O., Degani, G., 2007. Molecular DNA variation among Triturus vittatus vittatus (Urodela) from different breeding sites at the southern limit of its distribution. Acta Herpetol. 2 (2), 69–77.

Pearlson, O., Degani, G., 2008. The life history of *Triturus v. vittatus* (Urodela) in various habitats. Asiatic Herpetol. Res. 11, 91–95.

Pearlson, O., Blaustein, L., Snir, S., Goldberg, D., Degani, G., 2010. Molecular variation in triturus vittatus vittatus (Urodela) from breeding sites near the southern extremity of its distribution revealed by DNA sequencing of mitochondrial cytochrome b gene and control region. Curr. Herpetol. 29 (1), 11–22. https://doi.org/10.3105/018.029.0102.

Rehman, S., Parent, M., Storey, K.B., 2024. The mRNA N^6-Methyladenosine response to dehydration in *Xenopus laevis*. Animals (Basel) 14(22):3288. https://doi.org/10.3390/ani14223288.

Roundtree, I.A., et al., 2017. Dynamic RNA modifications in gene expression regulation. Cell 169, 7.

Sai, L., Li, X., Zhang, J., 2020. Transcriptome-wide m^6A methylation analysis in Xenopus laevis testes exposed to atrazine. Chemosphere 242, 125139.

Shi, Y., Ishizuya-Oka, A., Brown, D.D., 1998. Thyroid hormone regulation of adult intestinal stem cell development during Xenopus laevis metamorphosis. Dev. Biol. 201 (2), 139–152.

Wang, Y., Zhao, Y., Bollas, A., Wang, Y., & Au, K. F. (2021). Nanopore sequencing technology, bioinformatics and applications. In *Nat. Biotechnol.* (Vol. 39, issue 11, pp. 1348–1365). Nature Research. doi:https://doi.org/10.1038/s41587-021-01108-x.

Yaoita, Y., Brown, D.D., 1990. A correlation of thyroid hormone receptor gene expression with amphibian metamorphosis. Genes Dev. 4 (11), 1917–1924.

Yassouf, A., et al., 2025. Updated transcriptome assembly of *Pleurodeles waltl* and its application to regeneration studies. Front. Genet. 16, 119832.

Zhang, J., Li, C., Wang, Y., Zhu, J., 2023a. Dynamic m^6A modification of circRNAs in Xenopus testis development. BMC Genomics 24, 773.

Zhang, X., Li, X., Xu, Y., 2023b. m^6A-modified circRNAs in Xenopus laevis testes and their response to atrazine exposure. Genes Environ. 45, 5.